◆ Human Brain Mapping 15:231–246(2002) ◆
DOI 10.1002/hbm.10023

Timing and Connectivity in the Human Somatosensory Cortex From Single Trial Mass Electrical Activity

Andreas A. Ioannides,[1]* George K. Kostopoulos,[2] Nikolaos A. Laskaris,[1] Lichan Liu,[1] Tadahiko Shibata,[1] Marc Schellens,[1] Vahe Poghosyan,[1] and Ara Khurshudyan[1]

[1]*Laboratory for Human Brain Dynamics, BSI, RIKEN, Saitama, Japan*
[2]*Department of Physiology, Medical School, University of Patras, Patras, Greece*

Abstract: Parallel-distributed processing is ubiquitous in the brain but often ignored by experimental designs and methods of analysis, which presuppose sequential and stereotypical brain activations. We introduce here a methodology that can effectively deal with sequential and distributed activity. Regional brain activations elicited by electrical median nerve stimulation are identified in tomographic estimates extracted from single trial magnetoencephalographic signals. Habituation is identified in both primary somatosensory cortex (SI) and secondary somatosensory cortex (SII), often interrupted by resurgence of strong activations. Pattern analysis is used to identify single trials with homogeneous regional brain activations. Common activity patterns with well-defined connectivity are identified within each homogeneous group of single trials across the subjects studied. On the contralateral side one encounters distinct sets of single trials following identical stimuli. We observe in one set of trials sequential activation from SI to SII and insula with onset of SII at 60 msec, whereas in the other set simultaneous early co-activations of the same two areas. *Hum. Brain Mapping 15:231–246, 2002.* © 2002 Wiley-Liss, Inc.

Key words: magnetoencephalography; primary somatosensory cortex; secondary somatosensory cortex; magnetic field tomography; single trial; connectivity

INTRODUCTION

The question of variability of neuronal responses has a long history. The stochastic nature of spontaneous activity was demonstrated using unanaesthetized cat's isolated forebrains [Smith and Smith, 1964]. The relationship between single cell and local field potential has also been studied for a long time, for example, using a single microelectrode to record both the evoked potential and single cell responses with separate amplifiers tuned to appropriate frequency ranges. Using such a recording set up the probability of firing of a single cell in cat cortex could be sampled together with the local field potential after somatic or light flash stimulation. Despite the high variability from trial to trial such studies showed that, given enough stimulus presentations, a single cortical cell would generate a spike frequency distribution over time that duplicates the entire evoked potential including early and very late components [Fox and O'Brien, 1965]. The early pioneering studies lead to numerous investigations but relating single unit events and local mass electrical

*Correspondence to: Dr. Andreas A. Ioannides, Laboratory for Human Brain Dynamics, Brain Science Institute, RIKEN, 2-1 Hirosawa, Wako-shi, Saitama 351-0198, Japan.
E-mail: ioannides@postman.riken.go.jp
Received for publication 6 June 2001; accepted 9 November 2001

activity in single trials to behavior has proved a very difficult task. Recently progress is made in many different directions, thanks to advances in recording techniques and analysis methods. Simultaneously recorded activities in neurons in different brain areas have shown that accurate spike synchronization accompanied by discharge rate modulations with limited time-locking to external events may subserve cortical organization [Riehle et al., 1997]. In general, healthy, stable behavior is the outcome of electrophysiological brain activity endowed with high variability [Ghazanfar and Nicolelis, 2001]. To encode the time-variable properties of environmental stimuli and integrate them with past experience and ongoing activity sensory systems have evolved hierarchical as well as distributed processing [Felleman and van Essen, 1991; Iwamura, 1998; Zhang et al., 2001]. Individual activations at each sensory node are subject to local dynamics, specific feed-forward and feedback loops and brain-wide influences [Hendry et al., 1999; Mountcastle, 1998]. Understanding how stable sensory representations are produced and hence lead to perception remains a challenge for contemporary neuroscience [Albright et al., 2000]. Mountcastle reconciles the dynamic aspect of neuronal function with the constancy of perceptual outcome by postulating that variability is minimal at the early stages of cortical sensory processing [Mountcastle, 1998]. This important hypothesis, together with many other questions relating to the origin and role of variability, are difficult to test in practice. With traditional electrophysiological and hemodynamic brain imaging techniques it is not possible to unfold the sequence of events leading to perception for each stimulus presentation, because the responses to repetitive identical stimuli are averaged or integrated. Invasive recordings are also limited because the recordings are too local and in any case one can never be sure that all significantly active areas have been targeted. We use whole brain tomographic estimates of activity extracted from average and single trial (ST) magnetoencephalographic (MEG) signals to sample variability in its regional and global manifestation. It is well known that radial currents do not generate an MEG signal, so our analysis misses neuronal activity producing purely radial current density and its variability. Radial generators produce strong electroencephalographic (EEG) signal [Lopes da Silva and Van Rotterdam, 1999]. Accurate localization from EEG signals demands accurate description of the electrical properties of the medium between the generators and the electrodes because of the high sensitivity of electrical measurements to the details of conductivity and especially the blurring introduced by the high skull resistivity. In contrast accurate localization can be obtained from MEG measurements with simple models of conductivity, like the sphere model we use in this study.

We will be concerned with the human brain processing of somatic sensory information, which is served by several cortical areas: primary (SI) and secondary sensory (SII), posterior parietal areas (PPA) areas 5 and 7b, granular insular and retroinsular cortex [Hendry et al., 1999; Mountcastle, 1998]. SI itself is not a unitary area: located in the post-central gyrus it is comprised of four cytoarchitectonic areas receiving information via afferents from ventrobasal thalamus both cutaneous receptors (primarily areas 3b and 1) and deep receptors in muscles and joints (primarily areas 3a and 2) [Geyer et al., 1999; Paulesu et al., 1997; Romo and Salinas, 2001]. SII is located in the upper (parietal) bank of the lateral sulcus behind the insula and receives information from receptors on contralateral, ipsilateral and both sides of the body (with the extent of the latter case varying highly and up to 80% of responsive neurons in monkeys) [Whitsel et al., 1969], in a somatotopic organization, via afferents from the ventrobasal complex of thalamus [Burton and Sinclair, 2000; Kaas, 1990; Paulesu et al., 1997]. In this area two cortical fields, called SII and parietal ventral area (PV) have been distinguished in a wide range of mammals, including macaque monkeys [Burton et al., 1995; Krubitzer et al., 1995] and humans [Disbrow et al., 2000].

Anatomy allows the independent activation of SI and SII from thalamus (Jones, 1985), but also indicates hierarchical connections from SI to SII, because the

Abbreviations

a.u.	arbirtrary units
EDA	exploratory data analysis
EEG	electroencephalography
fMRI	functional magnetic resonance imaging
Las	left arm strong stimulation
MEG	magnetoencephalography
MFT	magnetic field tomography
MI	mutual information
NP	noise power
PPA	posterior parietal area
PV	parietal ventral area
Ras	right arm strong stimulation
RMA	robust moving average
ROI	region of interest
SI	primary somatosensory cortex
SII	secondary somatosensory cortex
ST	single trial
SNR	signal to noise ratio
SP	signal power

two areas have rich interconnections and most prominently SI has "forward" connections to SII of both hemispheres, whereas SII has "feedback" connections to SI of the same side and callosal connections with SI and SII of the other side [Felleman and van Essen, 1991]. Responsiveness of SII neurons in monkeys is decreased after surgical ablation of SI [Pons et al., 1992] but not during transient inactivation of SI [Zhang et al., 2001]. The later experiments present SI and SII as hierarchically equivalent areas receiving independent activations from thalamus. Monkey SI and SII neurons have been shown to encode this information synchronously using different encoding strategies [Nicolelis et al., 1998]. The distribution of work between the two areas certainly relates to the somatosensory submodality [Zainos et al., 1997], whereas the particular sensitivity of SII to selective attention or novelty [Mima et al., 1998], its largely bilateral inputs [Iwamura et al., 1994; Manzoni et al., 1984] and its association to sensorimotor integration [Huttunen et al., 1992] and tactile learning [Kawakami et al., 2001] present the SII area as somewhat higher-order sensory node than SI. In consistency to this notion, the receptive field responses in this system appear relatively later and increase in complexity as we move from SI areas 3 to 2, to 5 and then to area SII supporting the view that part of somatosensory information is serially processed from SI to SII toward increased sensory integration [Iwamura, 1998].

Magnetoencephalography (MEG) [Hari and Forss, 1999; Kakigi et al., 2000] and fMRI [Disbrow et al., 2001; Gelnar et al., 1998; Hamalainen et al., 2000; Ruben et al., 2001] studies identify many of these areas and demonstrate that in humans the cortical network activated by even simple somatosensory stimuli is complex and widely distributed. The activation in SI can be robustly identified first at about 20 msec, referred to as N20 and M20 in EEG and MEG respectively. The SII activation is identified best 70–100 msec after SI [Disbrow et al., 2001; Hari et al., 1984; Korvenoja et al., 1999; Shimojo et al., 1996; Simoes and Hari, 1999; Wegner et al., 2000], although few studies have also identified an earlier SII response [Karhu and Tesche, 1999; Korvenoja et al., 1999]. These studies rely on averaging and therefore miss some basic information regarding the relative time sequence and mutual dependencies of responses. Even within studies using just average signals there are important unsettled questions. Is sensory information reaching SI and SII via independent parallel thalamocortical volleys, or via serial activation of SI and SII [Hari and Forss, 1999; Kaas, 1990; Karhu and Tesche, 1999; Paulesu et al., 1997; Zhang et al., 2001]? What is the nature of interactions between ipsilateral SI and SII with contralateral SII [Disbrow et al., 2001; Karhu and Tesche, 1999; Manzoni et al., 1984; Simoes and Hari, 1999; Shimojo et al., 1996]? How plastic is the response in the sensory cortex [Ribary et al., 1999; Wegner et al., 2000]? When these questions are addressed the enormous variability evident in somatosensory responses at both the single unit and mass neuronal levels is ignored. This is reasonable in some cases, for example, in demonstrations of long-term reorganization as an adaptation to changes in sensory input [Elbert and Flor, 1999; Ribary et al., 1999]. In other cases variability may play some role, for example, when short-term plasticity in SII is examined [Huttunen et al., 1992; Karhu and Tesche, 1999; Wegner et al., 2000]. In an earlier study we demonstrated that ST responses to identical simple auditory stimuli formed distinct sets of responses with very robust distribution for each subject [Liu et al., 1998]. In this study, we identify ST responses in SI and SII elicited by intermittent median nerve stimulation in three volunteers. The ST activations from each region are separated into clusters by powerful pattern analysis and graph theoretical tools. Focusing the computationally intensive tomographic analysis to selected subsets of STs provides the means for extrapolation from what is regionally consistent to the corresponding global pattern(s) of activity. The regional activations show the expected spatiotemporal variability and reveal habituation in both SI and SII. The extrapolation to global dynamics reveals distinct and novel inter-regional interactions common across the three subjects.

MATERIALS AND METHODS

Data collection

Three healthy, normal right-handed male subjects (N1-3, ages 48, 52, 55) volunteered for the MEG experiment. Ethical committee approval was obtained from the host institution and subjects gave written consent before the experiment. Electrical pulses (duration 0.2 msec, inter-stimulus interval 1.0 sec) were applied respectively to the left and right median nerves at the wrist, at two levels. Weak (w) and strong (s) levels were defined by, $w = F + 0.25 \times (T-F)$ and $s = T + 0.25 \times (T-F)$ where F and T denote the level when the subject just felt the stimulus and when the stimulus induced a small twitch, respectively. In total four runs were recorded, one for each arm and level. The mean levels for weak and strong stimulation were 4.5 and 9 mA respectively. For strong (weak) stimulation 90 (270) repetitions were applied. The MEG signal was recorded in continuous mode, using CTF Omega whole head system (151 channels), with low-pass fil-

tering at 200 Hz and digitization at 1,250 Hz. The data were further high-pass filtered above 1 Hz before segmented into epochs from 200 msec before to 400 msec after the stimulus onset.

Source-reconstruction analysis of MEG signal

Magnetic field tomography (MFT) [Ioannides et al. 1990] was applied to the average signal of each run for each timeslice (0.8 msec) independently. In addition MFT solutions were computed for selected subsets of STs from each run, after the removal of oculographic and cardiac artifact using independent component analysis. The resulting current-density estimates provided the overall spatial distribution of instantaneous brain activity. Based on the maxima of MFT solutions for the average response to contralateral strong stimulation, regions of interest (ROIs) including the SI and SII in each hemisphere were defined. A radius of 1 cm was used for each ROI, which is conservatively large because it contained more than one of the tight foci seen in the MFT solutions. The direction of maximum current density at or close to the latency of the designated average peak was defined as the main direction. SOFIA, a spatially optimal fast method for extracting activations from the MEG signal [Bolton et al., 1999], was then used to compute for each time slice the integrals within the ROI of the local current density vector J and its projection along the main direction J_1. SOFIA's output for J_1 provided the response time-course of each ROI for *all* the STs. Pattern analysis of the derived ST-signals was performed independently for each ROI.

Pattern analysis of SOFIA-based ST-signals

Event definition and pattern extraction

A conventional estimator [Laskaris et al., 1997] was employed, providing the signal power (SP), noise power (NP) and signal to noise ratio (SNR) when a signal embedded in noise is observed over repeated trials. The resulting measurements revealed the existence of time-locked response of significant signal content in all cases apart from the signals from ipsilateral SI. For strong stimulation, the evoked response consisted of prominent deflections in the post-stimulus interval of the averaged ST signal. Each deflection was considered as a distinct event of the evoked response and a pattern conveying its time course was extracted. The range of the event-pattern was defined from the zero crossings around the peak in all cases apart from the early contralateral SI event where the two latency landmarks around the peak were estimated via optimal thresholding with the baseline. The same latency range was used to extract from each ST-signal corresponding event-patterns. Latency ranges, SP and SNR measurements within the range of each event are given in Figure 1.

Robust moving averaging

The changing dynamics were monitored as the run progressed using the technique of robust moving averaging, applied to ensemble windows of ST events defined around each trial [Laskaris et al., 1997]. The ensemble window for the i^{th} trial included the event pattern of the i^{th} trial and the event patterns of the (w-1)/2 preceding and (w-1)/2 following trials. A "k out of w" selective averaging on the i^{th} ensemble window of event patterns provided the estimate of the current state of each event. The clustering step delineated the most homogeneous subset of $k = 10$ patterns with its centroid providing a quasi-continuous quantifiable measure of the current state, which included its corresponding SP measurement.

Unsupervised classification of ST patterns

For each event one encounters very diverse ST-patterns, which very likely correspond to very different local processes. It is desirable to separate these ST-patterns into clusters, each containing similar patterns. The fuzzy c-means clustering algorithm was employed for organizing the ST-patterns of each event into three homogeneous groups [Zouridakis et al., 1997]. The output of the algorithm, after maximum membership defuzzification, was a list of labels denoting the group-membership of each ST-pattern. The clustering algorithm was applied after excluding 20% of patterns with the lower local point density to provide the grouping procedure with robustness against possible distinct or noise-contaminated patterns. The local point density is computed in the multidimensional space where the patterns resided [Laskaris and Ioannides, 2001].

Ordering of ST-patterns

The ST-patterns of a certain event were configured as points in R^p (p is the number of signal samples in each pattern) and the exploratory data analysis (EDA)-framework enabled the "natural" ordering of them [Laskaris and Ioannides, 2001]. After identifying the single pattern where the event was better portrayed, ranks were assigned to the patterns according to their

Subj. / ROI	N1			N2			N3		
Left SI	-41	-33	58	-43	-32	54	-57	-37	42
Right SI	42	-33	49	48	-30	49	55	-17	41
Left SII	-42	-7	24	-56	-6	27	-58	-29	16
Right SII	53	-7	8	64	-20	21	56	-11	16

Signal Power ($\times 10^{-22}$ a.u.) / SNR / [Pattern-range] peak-latency (msec)		cSIa		cSIb		cSII		iSII	
N1	Las	6.31	0.361	0.09	0.046	0.18	0.084	0.34	0.137
		[14-25], 23		[29-176], 33		[63-129], 70		[67-139], 79	
	Ras	0.30	1.7645	0.15	0.9651	0.96	0.486	0.14	0.094
		[17-28], 24		[22-64], 34		[50-111], 85		[76-149], 120	
N2	Las	30.27	1.109	2.05	1.113	1.56	0.864	1.05	0.2416
		[14-25], 21		[35-122], 44		[34-164], 96		[67-171], 106	
	Ras	74.4	0.563	1.72	0.596	2.24	0.819	0.66	0.171
		[17-25], 23		[29-116], 44		[60-146], 103		[72-162], 115	
N3	Las	8.44	1.406	0.19	0.218	0.29	0.317	36.63	0.6854
		[17-28], 26		[32-168], 48		[66-149], 80		[76-130], 85	
	Ras	44.60	1.392	39.61	1.045	55.76	1.34	0.32	0.26
		[18-28], 26		[32-153], 44		[63-140], 78		[72-148], 100	

Figure 1.

The top part shows the Talairach coordinates (mm) for the SI and SII of both hemispheres in the three subjects (N1, N2, and N3). The centers of four areas are defined by combining anatomical considerations with functional information from the MFT solutions. A spherical ROI of 1cm-radius is defined around each center and SOFIA is used to compute the activation within this ROI for *all* STs at each time slice. In the main (lower) part of the figure events are recognized in the SOFIA-based signals and the patterns associated with them are given by the tabulated parameters in the arrangement and colors defined in the top left cell. The top row of each cell shows the signal power (SP) in black and next to it the signal-to-noise (SNR) in blue (the SNR of an averaged event is 90 times higher). The bottom row of each cell shows the latency range and peak latency in red.

resemblance with the selected prototype (first in the ordered list). The first 10 patterns in the list were considered as the high-SP group, because the SP measurement restricted to this subset was always (3–6 times) higher than the one for the whole set. The ordering procedure was repeated after identifying the antipode, in the point-configuration, of the previous prototype. The first 10 patterns in the new ordered list were considered as the low-SP group.

Statistical analysis of MFT solutions

MFT was applied to each ST signal and the average in each pattern, for each other timeslice (1.6 msec)

independently. Statistical parametric maps (SPMs) were computed, for each subject and type (i.e., run, event identity, SP-level) of ST-subsets separately, based on the corresponding MFT solutions. For each source space point distributions of MFT moduli were formed from the STs of each ST-subset of each subject within 6.4 msec windows with centers at a step of 3.2 msec. The least significant *P*-value was assigned to each post-stimulus window after six-paired *t*-test comparisons each with baseline distributions from the prestimulus period (−190 to −70 msec). The SPMs of each subject, corresponding to a certain ST-subset type, were brought into a common Talairach space and statistically significant ($P < 0.05$ corrected) increases and decreases of activity across all subjects were identified within successive 9.6 msec windows. The resulting common SPM was then back-transformed to the coordinate system of one subject and overlaid with his MRI for display purposes.

Mutual information analysis of SOFIA ST-signals

A detail description of mutual information (MI) analysis for quantifying the linkage between areas based on ST-signals can be found elsewhere [Ioannides et al., 2000]. The MI between two brain areas was computed first for each ST from the respective SOFIA-based ROI activations. Specifically the Renyi generalized mutual information [Renyi, 1970], with Renyi parameter $q = 4$, was computed between two 60-msec windows, one for the first ROI (ROI_1) and one for the second ROI (ROI_2). The center latency of the window from ROI_1 is denoted by t, while the center latency for ROI_2 is $(t + \tau)$ allowing for a delay τ. A positive (negative) τ indicates that ROI_1 leads (follows) ROI_2. The computation was performed for each allowed (t, τ) pair, building a map of MI in the (t, τ) plane across ST. The resulting MI-maps were obtained either from the whole set of STs or from ST-subsets of the same type.

Overview: why and how the methods are applied

The basic unit of MEG data is the signal value recorded by a single sensor (channel) at one point in time (timeslice) in one ST. The latency (time from the onset of the stimulus) endows a common time-label that can be used for averaging across STs. A change in source activity generates a change in the magnetic field that is captured by each sensor instantaneously, because the propagation from the source location in the brain to the sensing coils proceeds with the speed of light. The instantaneous MEG signal is the linear sum of contributions generated by changes in source activity in multiple sites at just that one timeslice. In general, in each ST a different set of generators contributes to the MEG signal at any latency. Only a small subset of generators is activated at similar latencies with similar strength in either all or even a subset of STs. The signal from generators that are activated in the most consistent way with respect to the stimulus onset is enhanced relative to the rest by averaging. What appears as a sequence in the average does not necessarily correspond to a true sequence in STs, it can very easily be contributions gathered along from different STs and superimposed on a single trace. The individual generators in the set of STs are disentangled using the set of methods described above, each addressing a different aspect of the problem. MFT extracts from signals estimates of activity in both space and time in a tomographic format, without any assumptions about the number and form of the generators. MFT is applied twice, first on the average signal to identify approximate foci of activity. SOFIA is then used to generate time courses for *all* STs from the circumscribed areas identified by MFT, followed by pattern analysis applied to the resulting ST regional activations to identify temporal trends and to group similar STs together according to local event-patterns. MFT is applied for the second time to each ST within each selected homogeneous group at each timeslice. Post-MFT statistical analysis and MI are then used respectively to produce precise localization for the generators and to investigate the information flow between the identified areas for each homogeneous group of STs.

RESULTS

We used MFT to extract tomographic estimates of activity from the average and sets of ST signal. In each subject we identified ROIs corresponding to SI and SII and for each ROI we computed the time course from the MFT average and ST solutions for each condition. Both strong and weak stimulation induce phase reorganization and a slight amplitude increase in the low frequency components (below 20 Hz) of SI and SII activations. Only the early part of contralateral SI activation, corresponding to the M20 response to strong stimulation, is characterized by stimulus evoked high frequency components (above 20 Hz). We emphasize below the results from the analysis of ST responses to strong left and right median nerve stimulation, which are denoted hereafter as Las and Ras, respectively. A wide frequency band (1–200 Hz) was used, because even if high frequency SI activity initiates changes,

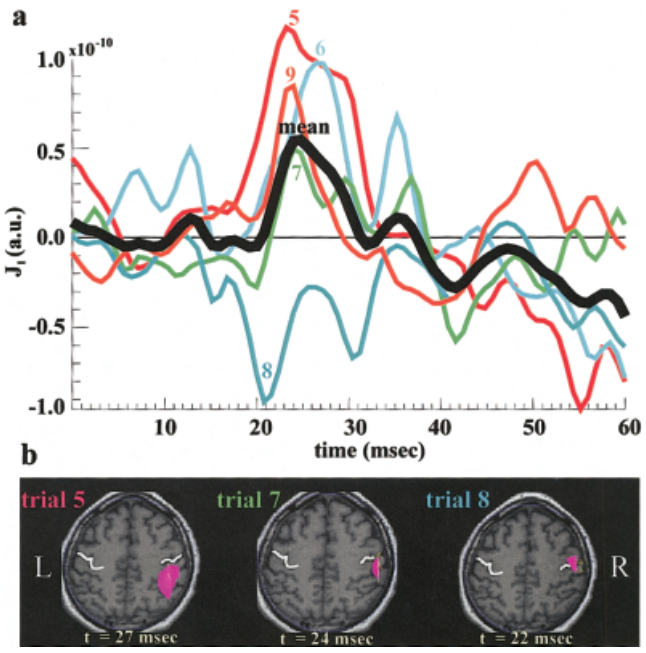

Figure 2.

The MFT solutions for 5 STs (Trials 5–9) from strong left median nerve stimulation. (**a**) The response time courses from right SI ROI, together with their average (heavy black line). (**b**) Instantaneous distribution of activity in an axial slice through the SI ROI at the latency with strongest activity between 20 and 30 msec. The heavy white line marks the central sulcus. The color-shaded areas indicate regions with activity above 70% of the instantaneous maximum (IM) in activity over the slice, while the arrows indicate the current flow directions. For Trial 5 the first IM is identified at 24 msec, in the fundus of the sulcus (not shown) and a second IM with a higher value is encountered later, at 27 msec, at the PPA (left figurine). For Trials 6,7,9 the IM in activity remains for a long period just behind the central sulcus; the middle figurine shows the overall maximum at 24 msec for Trial 7. For Trial 8 the strongest activation is at 22 msec, in front of the central sulcus with current density direction along the motor strip (right figurine).

these changes may be expressed in another area at a different frequency range. Figure 2 uses MFT solutions for five successive STs, to demonstrate that variability has both temporal (Fig. 2a) and spatial aspects (Fig. 2b). There are three distinct spatial distributions in this set (Fig. 2b) and there is enough of a hint in the SI time course morphology (Fig. 2a) to suggest a relationship between the spatial and temporal variability: single trials with peak activity identified just behind the central sulcus have similar timecourses of SI activation in terms of sign, latency of peak and its morphology between 20 and 30 msec (e.g., Trials 6, 7 and 9), which is different from the timecourse of SI activation for the trials that localize either more posterior (Trial 5) or in the motor strip (Trial 8). The examples displayed in Figure 2 are typical of the entire set of STs. Latency and amplitude jitter of the regional responses and variability in the spatial distribution were common to all ROIs and subjects. These observations suggested that averaging across trials might mix together contributions that logically should be studied separately.

The objectives of our work were to describe in a quantifiable way the spatial and temporal aspect of variability, to control variability within selected ST groups and hence study with better statistics the activity within homogeneous groups of STs. Computing the tomographic MFT solutions of all STs requires enormous processing power and disk space so we used the less demanding SOFIA to target the ST responses from SI and SII ROIs of both hemispheres. Significant events were recognized in the response time course and pattern analysis principles were employed to analyze the morphology of these events on a trial-to-trial basis. Figure 3 demonstrates, for Subject N1, the intermediate steps for the ROI definition, the computation of activity within each ROI for the first 10 STs of strong right median nerve stimulation and the detection of significant response events from the corresponding average of 90 STs. Figure 1 lists for all subjects the Talairach coordinates [Talairach and Tournoux, 1988] of the SI and SII ROIs and their time course characterization in terms of SP, SNR, latency and range of the significant events. Only the strong left/right median nerve stimulation runs are listed. For each run, four different events were recognized, an early and a late response for contralateral SI (cSIa and cSIb), contralateral-SII (cSII) and ipsilateral-SII (iSII). Despite the large variability at ST-level and the inter-subject differences in SNR, the peak-latencies and ranges of these four main events in the average response were consistent across the three subjects.

As a first approach to analyze the response variability, the technique of robust moving averaging (RMA) [Laskaris et al., 1997] was used to track the evolution of each response-event within a run across *all* STs. Monitoring the waveforms produced by RMA with a sliding window of 15 trials revealed vividly the non-stationary character of the response generation mechanism, but did not show any switching in the response mode. Because changes in strength were the main component of the monitored event-variation, the strength dynamics were studied further. A SP-estimate was derived via the RMA allowing the strength of each event to be monitored as a function of stimulus repetition number. The results, pooled together for the three subjects are displayed in Figure 4 and they show event-related habituation for both iSII and cSII in each

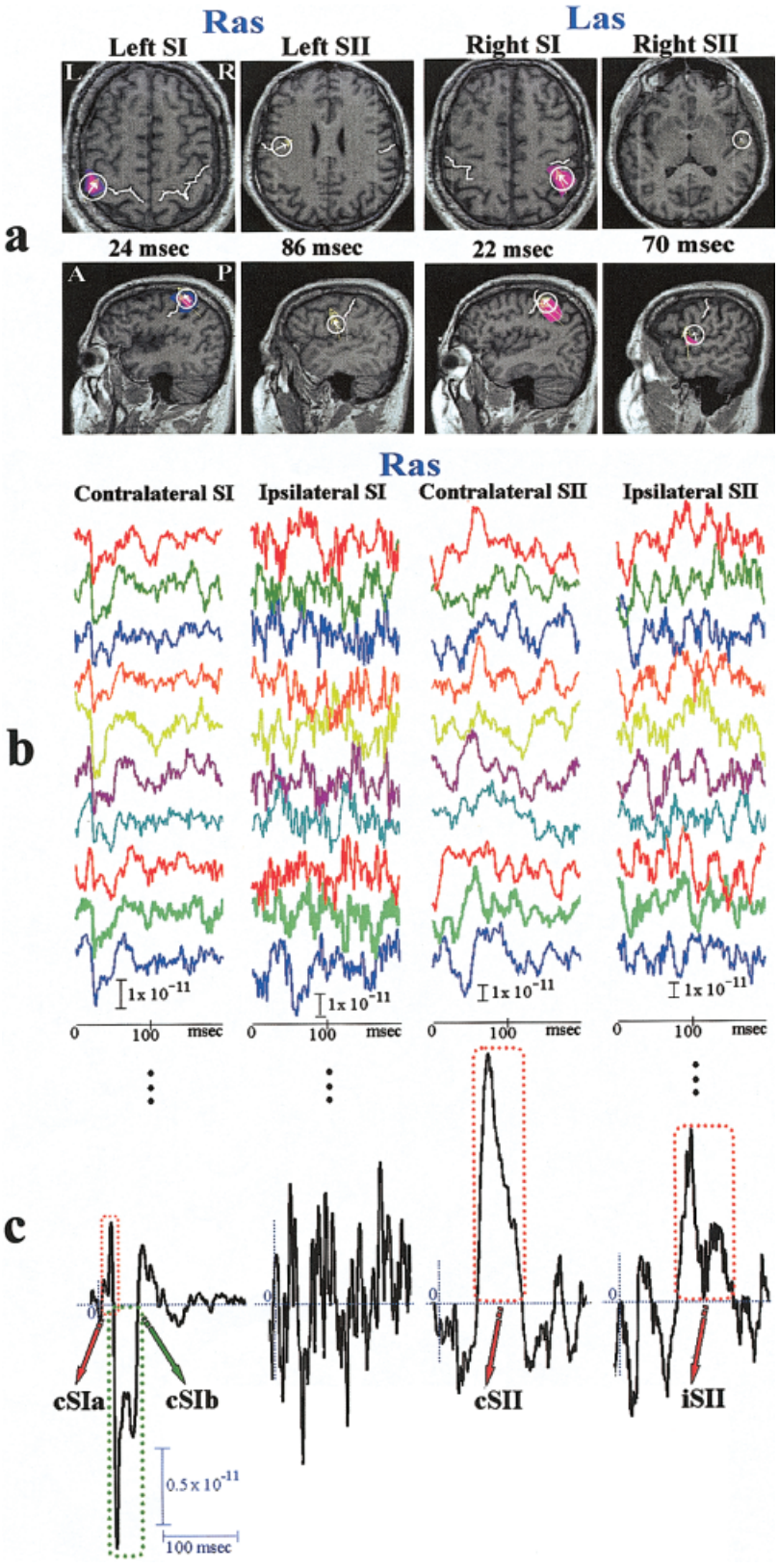

Figure 3.
Steps leading from the MEG signal to the detection of significant events in somatosensory cortex response. (**a**) The MFT solutions for the average response to Ras (Las) stimulation are used to define spherical ROIs containing the left (right) SI and SII areas. (**b**) The SOFIA estimates of ST-activity within the four ROIs for Ras. (**c**) Events are recognized from the morphology of the average of SOFIA-based ST-signals, as highlighted by the dotted squares.

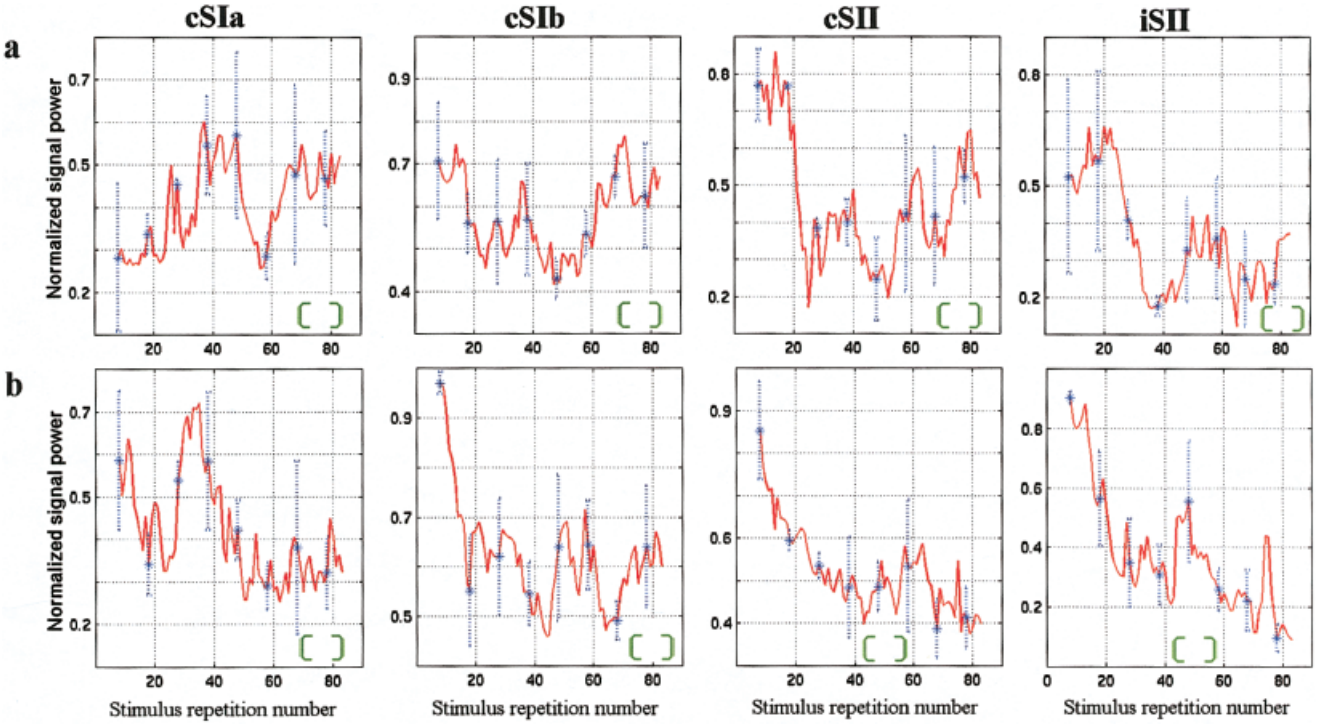

Figure 4.

Changes in SP content as a function of trial number for each event are derived from robust moving averaging (RMA). (**a**) Las-stimulation. (**b**) Ras-stimulation. The grand-average across the three subjects was computed after the individual sequences of SP-estimates were scaled so that the maximum was unity. In the same graph, the corresponding standard deviation is marked as a blue vertical dash line to indicate the extent of inter-subject variability. The green envelope serves as an indicator of the RMA window-width. The figure shows resurgence of activity (best seen in SI) and rapid habituation (best seen in Ras cSIb and all SII cases).

run and for the cSIb in Ras only. The habituation is especially rapid for the SII responses in the case of weak stimulation (not shown) with SNR reaching very small values within the first 20–30 trials. The change in SP is non-monotonic, with habituation intermittently interrupted by fairly long bouts of SP recovery, which often gives way to stronger habituation. The Las cSIa-event provides an example of a particularly strong increase of activity later in the run with no obvious early habituation possibly because the level of activity in the early STs is low.

The delineation of events in each ROI (Fig. 5a) and the subsequent tracking of their strength along the trial-to-trial dimension gave rise to multiple graphs (Fig. 5b). These graphs provided some evidence for coupled dynamics in a few cases (e.g., between cSII and iSII in Fig. 5b), but they were limited in their general use for studying functional linkage between areas. The restriction to amplitude dynamics and long time scales, posed by the type of measurement being tracked and the RMA window-width respectively, made these graphs poor tools for quantifying/tracing inter-area covariations. To alleviate these restrictions a clustering algorithm was employed to split the ST event-patterns into groups and the membership-label of each pattern was plotted as a function of stimulus repetition number (Fig. 5c). The strength of the event produced the only striking morphological differences between clusters. Among the four main events, the cSIa and cSII were the ones associated with the clearest event-strength related self-organization of patterns as can be seen, for example, in Figure 5d. Possible covariations between two events from different ROIs was sought as coherence in the grouping of STs and quantified by the fraction of common elements in the two label-lists (a randomization test [Hubert and Schultz, 1976] was used to compute chance levels). This study provided evidence for occasional and weak functional coupling between areas. The overlapping character of the derived clusters and the time limits imposed by the duration of each event were possible reasons why stronger coupling, if present, could have escaped detection. To advance the grouping procedure contextual information was incorporated to identify well separated groups of event-patterns and the possibility that these groups could correspond to dis-

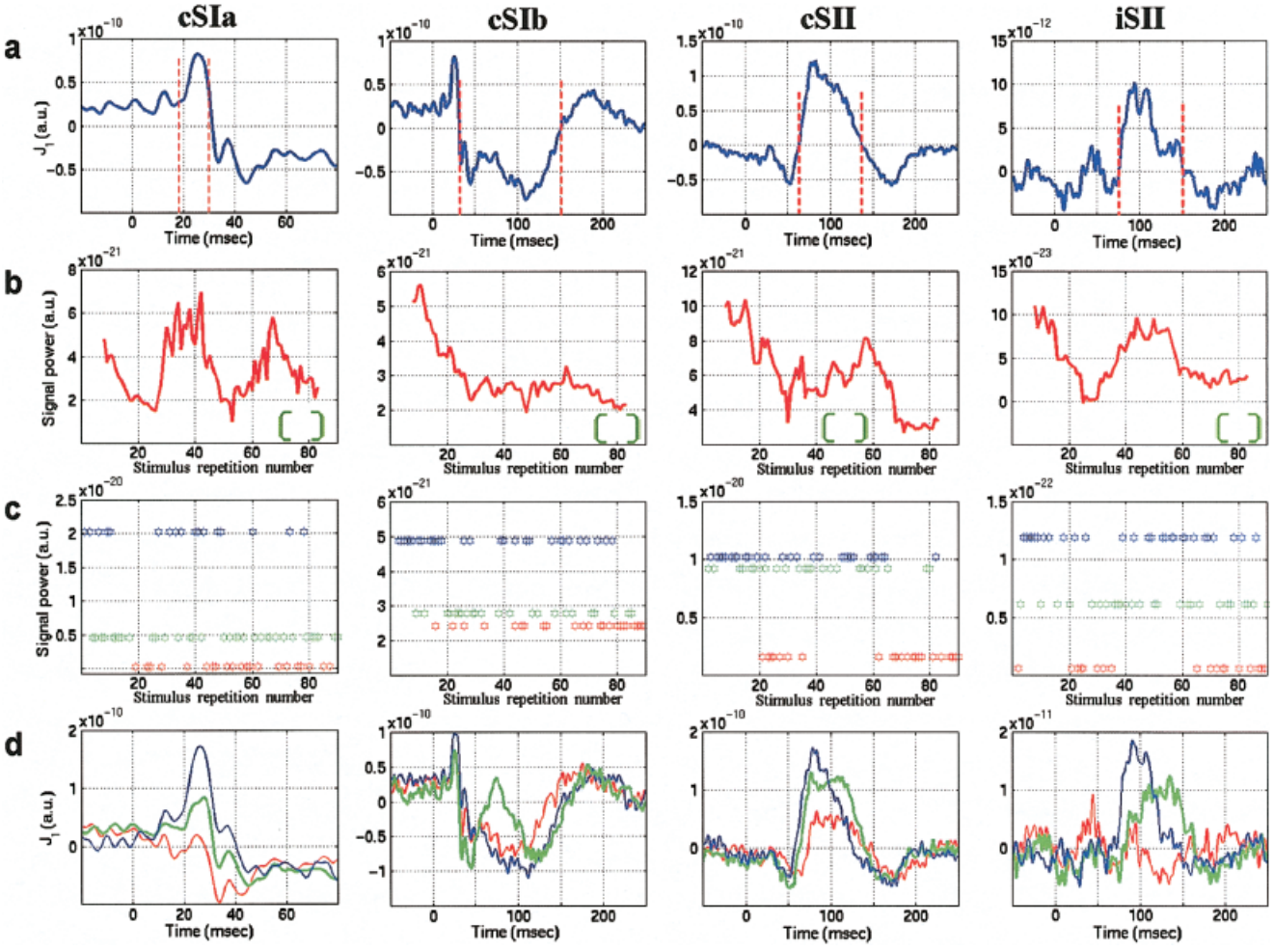

Figure 5.

Unfolding the response dynamics from the averaged signal in Ras for subject N3. (**a**) Definition of event range based on the average signal. (**b**) Evolution of event-SP along the trial-to-trial dimension. (**c**) Group membership of STs after unsupervised classification into three groups; the clusters produced by the fuzzy c-means algorithm were sorted according to the within-group SP-measurements and their members are denoted with asterisks at the corresponding SP-level. (**d**) The cluster centroids, plotted in the same color as the cluster members in (**c**), provide a decomposition of the average event into three wavelets (sub-averages).

tinct functional patterns was explored during extended time ranges.

The exploratory data analysis [Laskaris and Ioannides, 2001] was employed to identify via ordering two mutually exclusive groups in the ensemble of ST-patterns of each event. The first group was characterized by high SP because it emphasized the contribution from the generators mainly responsible for the event, whereas the second group reflected possible systematic complementary activation and was characterized correspondingly by low SP (Fig. 6). Hereafter the pair of ST-subsets corresponding to the identified groups is referred to as high/low SP-subset with the associated event added in a parenthesis. We note that the SP is an intrinsic measure of each cluster and it does not involve comparison with the average. It follows that although the high SP cluster is expected to enhance features of the average, other clusters might emerge with very different properties. The physiological rationale is that different clusters should correspond to different local processes, whereas STs within each cluster should correspond to similar local processes. As we will see this expectation is confirmed by the analysis.

We reasoned that if similarity between event-patterns reflects uniformity in activation of the corresponding neural circuitry it should be possible to use it as a bridge between strictly local and global, distributed dynamics. The subset of STs corresponding to the most promising couples (e.g., in terms of high SP

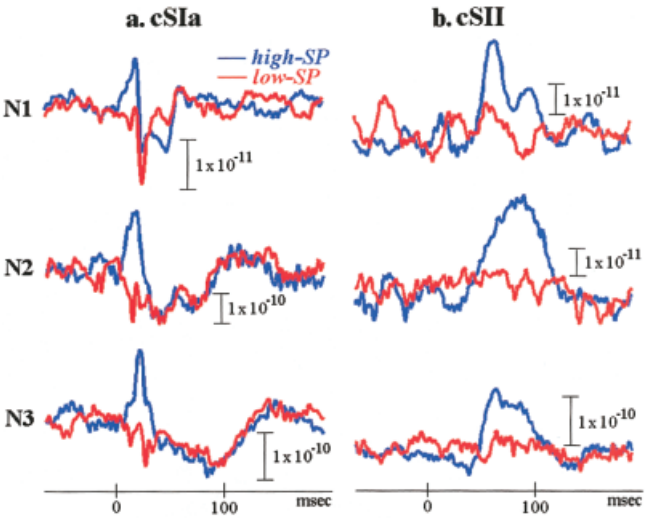

Figure 6.
Contrasting sub-averages of STs from high and low SP event-pattern groups delineated via EDA-based ordering in Ras of all subjects. (**a**) Early left SI response for groupings based on the cSIa-event. (**b**) Left SII response for grouping based on the cSII-event.

content) should contain strong signatures of neural activity over extended time periods and throughout the whole brain concomitant to the local changes that are directly responsible for the event-pattern subset. The MFT solutions were computed for each ST in each subset defined by the cSIa and cSII events (the ones most likely to produce distinct functional modes). Statistically significant changes were computed between pre- and post-stimulus activity for each set and the ones common to all subjects identified. Statistically significant increase in activity across all three subjects was identified only in cSI-area within the first 30 msec for high-SP(cSIa) subset in Ras (Fig. 7a), and in two nearby foci for high-SP(cSII) subset, one in the cSII proper and the other in the adjacent insula (Fig. 7b). No other common areas of increase or decrease in activity were identified for these two high-SP subsets, or anywhere for the corresponding low-SP subsets of the same run (Ras). In the statistical analysis of individual subjects (not shown) highly significant decrease in activity was identified in the left insula for subject N1 and in the right parietal area for the other two subjects in the period of 73–89 msec in the low-SP(cSII) subsets.

The same ST-subsets were also used to study inter-area communication, by computing the MI between pairs of ROIs [Ioannides et al., 2000]. In the present case MI provided a non-linear measure of (lagged) covariations in SI and SII of either the same or opposite hemisphere with very fine temporal resolution. The MI-maps computed from all STs showed no systematic behavior across subjects. In contrast, the MI-maps computed from SOFIA STs belonging to the homogeneous high or low SP subsets revealed patterns that were common across subjects both in terms of localization and form of communication. Of specific interest was the contrast of communication modes between cSI and cSII areas, for the cases that the pair of subsets had been defined based on the cSII-event. The high-SP(cSII) subset gave rise to common islands of high MI at the beginning of the cSII-event, 60–70 msec on the left hemisphere (Fig. 7c), and 50–55 msec on the right (not shown). The delays were 20 and 40 msec, which corresponded to start of initiating events in cSI at 40 msec (i.e., end of cSIa-event on left hemisphere) and 15 msec (i.e., beginning of cSIa-event on the right hemisphere). The low-SP(cSII) subsets also produced common islands of high MI: for both right and left median nerve stimulation these islands corresponded to early and long co-activation of cSI and cSII areas (20–60 msec). During the first 10 msec of coactivation, the common events lined with constant delay of 2 msec, with SI leading on the left hemisphere (Fig. 7d) and SII leading on the right (not shown).

DISCUSSION

Figure 7 demonstrates how ST tomographic information can be used to identify activation patterns in SI and SII common across subjects. We emphasize that the results displayed in the figure were obtained from post-MFT statistical analysis using data from three subjects restricted to homogeneous sets of STs from each subject. These homogeneous sets were selected by objective methods from the full set of data that had substantial variability from trial to trial. To arrive at the final result many intermediate steps were taken. The first step was the preliminary identification of the areas and activation patterns using MFT solutions extracted from the average signal. The SI and SII ROIs defined in this way were used for the SOFIA estimates of activity for *all* STs. The original ROI identifications suffered from the limitations of the average, especially in terms of localization: the identified locations were not exactly right, especially for SII. The average signal contains contributions from different sets, some no doubt with activations in different areas. The ROI definitions were nevertheless accurate enough to produce SOFIA ST estimates with enough signal content for the pattern analysis tools to define compact clusters. The re-introduction of tomographic analysis and subsequent statistics and mutual information analysis

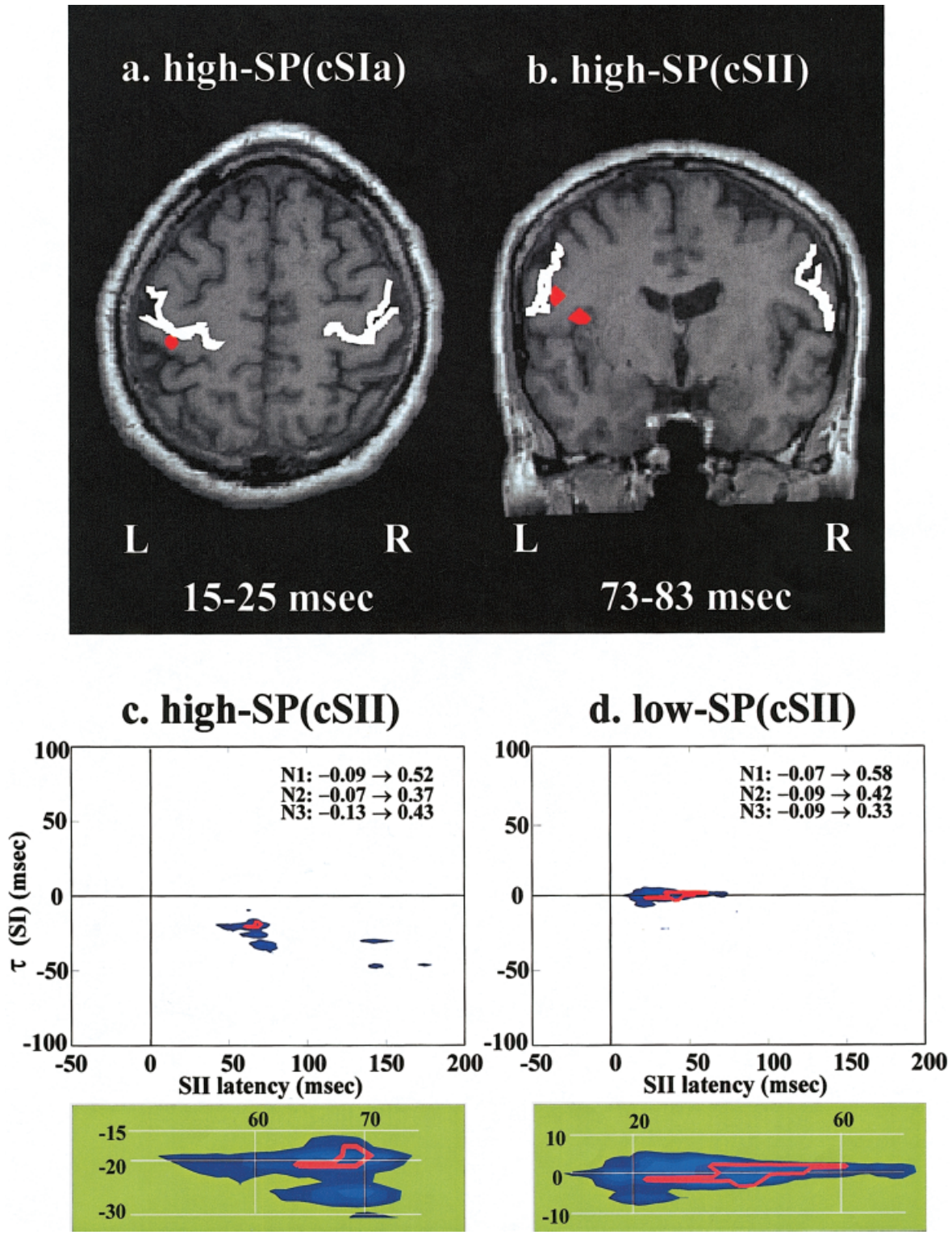

Figure 7.

Across subjects consistency of activity distribution (upper panel) and connectivity between areas (lower panel) within selected ST-subsets in Ras. (**a**) High-SP(cSIa) subset: the only region with common significant increase in activity ($P < 0.05$ corrected) across the three subjects is just behind the contralateral (left) central sulcus at the level of the Omega knob [Yousry et al., 1997]. This activity is seen in two successive post-stimulus windows covering the latency range 15–31 msec. (**b**) High-SP(cSII) subset: two nearby areas are identified, the contralateral SII and the adjacent superior part of insula cortex in the window 73–83 msec. Only the insula activation survives in the next overlapping window (79–89 msec). (**c**) High-SP(cSII) subset: the blue shade shows areas where the grand-average of the MI across the three subjects is high. The individual MI-maps are re-scaled so that the maximum is 1 and a red-contour bounds the area in the (t, τ) plane for which all re-normalized MI-maps are above 0.5. The well-defined overlapping region is enlarged and shown in the green shaded panel below. (**d**) Low-SP(cSII) subset: the same as (c). In (c) and (d) the range of MI values in the (t, τ) plane for each subject (N1, N2, and N3) are printed in text.

was applied to homogeneous sets of STs. As anticipated a distinct neuronal network corresponded to each set, enabling the transition from strictly regional analysis to global dynamics. The global detail extracted in this way extended over all brain regions, except of course magnetically silent regions or ones generating very little MEG signal. At the local level habituation was identified in both SI and SII, often interrupted by resurgence of strong activations. The identified networks differed significantly in their interaction mode on the left and right hemisphere. The activations in SI and SII and their interactions in each hemisphere were reproducible in the three subjects we have studied. These results taken together with recent studies of single trial dynamics of cortical stimulus representation during categorization [Ohl et al., 2001] suggest that response variability is physiologically relevant and relates to behavioral choices.

We do not know if neuronal mechanisms shown to cause habituation in simple nervous systems [Bailey et al., 2000] also apply to human brain [Christoffersen, 1997; Thompson and Spenser, 1966]. Although SII responses after 100 msec have been shown to be very sensitive to regular inter-stimulus intervals up to 10 sec long [Mauguiere et al., 1997], no such sensitivity was observed for SI responses [Hari et al., 1984; Huttunen et al., 1992; Wegner et al., 2000]. Omitting a stimulus has been shown to enhance the response to the succeeding stimulus only for SII responses after 100 msec, but not in SI or for the earlier (20 and 40–60 msec) SII responses [Karhu and Tesche, 1999]. We document here that all strong activations show changes in activity with long time constants. The event patterns changes on the contralateral side in late SI (as defined in Fig. 1) and in SII are consistent with habituation, but before we attribute them to habituation we must consider the alternative explanations, namely random trial fluctuations or changes in vigilance. We emphasize in this context that we have quantified changes using sensitive but also robust methodology. We have first identified the event patterns that stand out in the SOFIA based ST estimates of activity from SI and SII, and for each trial we have computed their latency range, SP and SNR. The changes for each event pattern were computed for each trial by considering a window of 15 trials at a time, centered on the target trial. Note that the measure of SP was very robust because it was computed from the 10 most representative trials in each window so that a few outlier trials would not have any effect. Thus the use of a homogeneous set of 10 trials in each window limited the effect of random trial fluctuations. Attention has been shown to modulate SII responses [Hoechstetter et al., 2000; Mauguiere, 1997; Mima et al., 1998; Steinmetz et al., 2000]. For the strong stimulation case, which we have studied here, the runs were kept short, less than 2 min. We have instructed our subjects to avoid changes in vigilance and although vigilance may change over the 2 min, we expect such changes to be sporadic and rare. Changes in vigilance are expected to affect both SI and SII simultaneously. In our data we have observed interactions among sensory areas rather than global changes. We therefore conclude that although changes in vigilance level cannot be excluded in theory, they are unlikely to be the main cause of the observed changes. Habituation in SI and SII remain the most plausible explanation especially for the strong changes identified in Figure 4; late contralateral SI on the right hemisphere (as defined in Fig. 1) and all SII responses. Very rapid habituation and rebounds of activity may be the reason why habituation was not evident in all cases (e.g., cSIa-event in Fig. 4a) and why it had escaped detection for SI responses in earlier studies where successive sets of 30 trials were used [Wegner et al. 2000].

Our data show that plasticity, which has been well documented as reorganization of representation maps after lesions and other long-term changes in sensory receptor activation starts at the earliest stage of somatosensory processing within seconds of repeating identical stimuli. Our results therefore do not support the assertion that sensory responses in the early stages of cortical processing should not vary [Mountcastle, 1998]. Constancy of perception could instead be sought in brain mechanisms compensating for variability. The effort to gather consistent results proving that variability exists is clearly a difficult, if not an impossible task. In the present work by using the robustness against random fluctuations of the SP measure derived from robust averaging method, we extracted significant, non-random changes along the trial-to-trial temporal axis. We note that what appears as inconsistency in the results and the trial variability is only expected when studying nodes in a distributed system. We have recently demonstrated that what appeared as random variability in activity in the fusiform gyrus in an object and face recognition task was in reality a reflection of an ingenious way of tackling a complex task by segregation of cortical processing in space and time [Ioannides et al., 2000].

Our study is relevant to the discussion regarding serial hierarchical processing and parallel distributed processing at the first cortical stages of the somatosensory system [Mountcastle, 1998]. Support to the serial activation hypothesis has been given by studies claiming only late (>60 msec) responses in SII with MEG

[Disbrow et al., 2001; Mauguiere et al., 1997; Mima et al., 1998; Simoes and Hari, 1999]. Other recent studies, also using averaging [Karhu and Tesche, 1999] report simultaneous early (20–30 msec) responses in cSI and cSII. Our results suggest that all activation modes available from anatomy may be used at different times. The mode seen as activity in cSII after 20 msec after strong activations in cSI (Fig. 7c) can be considered as functional support to the anatomical evidence of forward projections from SI to SII in the "hierarchical" manner [Felleman and van Essen, 1991]. A latency difference of 20 msec, however, does not exclude an indirect link between SI and SII. The evidence for a short latency difference between the activations in cSI and cSII (Fig. 7d) acquires significance in the light of animal experiments suggesting that such "reentrant" activation is a prerequisite for conscious perception of touch [Cauller and Kulics, 1991; Jackson and Cauller, 1998]. Such cSI and cSII activations are consistent with a monosynaptic gating function rather than autonomous activations. We are not aware of single unit studies examining the interactivity between SI and SII, but a proportion of pairs of neurons in these areas have been shown to fire synchronously within a range of 3 msec in the cat [Roy et al., 2001]. In the rat somatosensory cortex, a spike timing precision code of at least 2.5 msec is used to convey information about whisker location [Panzeri et al., 2001]. Interestingly in the present study the short lead of cSI occurred only in the left hemisphere (Ras) of all three (right-handed) subjects, whereas in the right hemisphere cSII was leading (Las). It is probably best to summarize our results without insisting on a dichotomy in terms of serial and parallel modes. We can state instead that ST responses separate in distinct and opposite clusters from a SP point of view, showing that across a sequence of identical stimulations very different modes of processing are present. One mode wins at the expense of the other in different STs. Averaging STs from such different clusters is not likely to improve SNR but only mix together contributions that must be treated separately.

The results presented here show that a strictly local view of the dynamics is not enough. To the ongoing activity [Arieli et al., 1996] and the local mesoscopic distribution of activity [Tsodyks et al., 1999] one should add the indirectly evoked inputs from other sensory areas of the same or the other hemisphere, which have been activated previously by the same stimulus, usually via sub-threshold synaptic depolarizations or inhibitions. Somatosensation, like vision [Bullier and Nowak, 1995] and hearing [Recanzone, 2000], is therefore too complex to be considered as based entirely on serial or parallel activations. Even within the seemingly sequential activations revealed by the MI analysis of the activations of the high-SP(cSII) subsets, the sequence from cSI to cSII on the left hemisphere suggests that some process is completed in cSI before cSII is activated on the left, whereas on the right the sequence initiation in cSII begins as soon as SI is activated. Thus, whether somatosensory information is processed serially, in parallel, or somewhere in between is not only dependent on the modality activated (touch more serial and pain, temperature and vibration more parallel) and the task performed [Zainos et al., 1997], but also depends on the time of activation, on short lasting plasticity phenomena as habituation and possibly on which hemisphere is involved.

In a recent work dealing with ST variability, it is suggested that correlations within and across hemispheres at the level of neurons are prominent when the local field potential oscillated in the gamma frequency with the variability in the spontaneous activity translating the functional architecture of cortical-cortical connections into column specific excitability fluctuations [Fries et al., 2001]. In another recent study, it was shown that as the sorting of auditory stimuli into categories emerges the sudden change in an animal's learning is accompanied by a change in the dynamics of cortical stimulus representation [Ohl et al., 2001]. In the present study we have shown that at the mass electrophysiological level different modes of covariation emerge when the response variability is analyzed without forcing all responses into one common set. Despite the highly overlapping nature of the neural circuitry, it is possible to cluster the ST responses into homogeneous sets and "pick up" the network corresponding to each cluster by one of its nodes. Although ironic, dealing with the ever-present variability as a prerequisite for identifying common activity patterns across different individuals and hemispheres, is not altogether surprising, given that the coherence of the living state is born and maintained in flux.

CONCLUSION

The results presented here taken together with other recent studies [Ioannides et al., 2000; Ohl et al., 2001] show that the underlying systematic behavior behind the apparent variability in local single trial activity can be accessed with sophisticated but well-defined methods. Quantification of similarity and dissimilarity between regional activation patterns leads to clustering that is meaningful physiologically and behaviorally. We have shown specifically that identical simple me-

dian nerve electrical stimulations produce cortical responses in SI and SII that fall in distinct clusters. Just like in the auditory system [Liu et al., 1998] it appears that averaging produces a sandwich of histories [Liu and Ioannides, 1996]. Connectivity between areas derived from the average signal often is just a revisionist mirage because activations in different modes from different sets of STs are overlaid. The sequence within each distinct cluster of homogeneous STs reveals a consistent connectivity across the three subjects.

REFERENCES

Albright DT, Jessel TM, Kandel ER, Posner MI (2000): Neural science: a century of progress and the mysteries that remain. Neuron 100:S1–S55.

Arieli A, Sterkin A, Grinvald A, Aertsen A (1996): Dynamics of ongoing activity: explanation of the large variability in evoked cortical responses. Science 273:1868–1871.

Bailey CH, Giustetto M, Huang YY, Hawkins RD, Kandel ER (2000): Is heterosynaptic modulation essential for stabilizing Hebbian plasticity and memory? Nat Rev Neurosci 1:11–20.

Bolton JPR, Gross J, Liu LC, Ioannides AA (1999): SOFIA: spatially optimal fast initial analysis of biomagnetic signals. Phys Med Biol 44: 87–103.

Bullier J, Nowak LG (1995): Parallel vs. serial processing: new vistas on the distributed organization of the visual system. Curr Opin Neurobiol 5:497–503.

Burton H, Fabri M, Alloway K (1995): Cortical areas within the lateral sulcus connected to cutaneous representations in areas 3b and 1: a revised interpretation of the second somatosensory area in macaque monkeys. J Comp Neurol 355:539–562.

Burton H, Sinclair RJ (2000): Attending to and remembering tactile stimuli: a review of brain imaging data and single-neuron responses. J Clin Neurophysiol 17:575–591.

Cauller LJ, Kulics AT (1991): The neural basis of the behaviorally relevant N1 component of the SS-evoked potential in SI cortex of awake monkeys: evidence that backward cortical projections signal conscious touch sensation. Exp Brain Res 84:607–619.

Christoffersen GR (1997): Habituation: events in the history of its characterization and linkage to synaptic depression. A new proposed kinetic criterion for its identification. Prog Neurobiol 53: 45–66.

Disbrow E, Roberts T, Krubitzer L (2000): Somatotopic organization of cortical fields in the lateral sulcus of Homo sapiens: evidence for SII and PV. J Comp Neurol 418:1–21.

Disbrow E, Roberts T, Poeppel D, Krubitzer L (2001): Evidence for interhemispheric processing of inputs from the hands in human S2 and PV. J Neurophysiol 85:2236–2244.

Elbert T, Flor H (1999): Magnetoencephalographic investigations of cortical reorganization in humans. Electroencephalogr Clin Neurophysiol 49(Suppl):284–291.

Felleman DJ, van Essen DC (1991): Distributed hierarchical processing in the primate cerebral cortex. Cereb Cortex 1:1–47.

Fox SS, Obrian JH (1965): Duplication of evoked potential waveform by curve of probability of firing of a single cell. Science 174:888–890.

Fries P, Neuenschwander S, Engel AK, Goebel R, Singer W (2001): Rapid feature selective neuronal synchronization through correlated latency shifting. Nat Neurosci 4:194–200.

Gelnar PA, Krauss BR, Szeverenyi NM, Apkarian AV (1998): Fingertip representation in the somatosensory cortex: an fMRI study. Neuroimage 7:261–283.

Geyer S, Schleicher A, Zilles K (1999): Areas 3a, 3b and 1 of human primary somatosensory cortex. Neuroimage 10:63–83.

Ghazanfar AA, Nicolelis MA (2001): Feature article: the structure and function of dynamic cortical and thalamic receptive fields. Cereb Cortex 11:183–193.

Hämäläinen H, Hiltunen J, Titievskaja I (2000): fMRI activations of SI and SII cortices during tactile stimulation depend on attention. Neuroreport 11:1673–1676.

Hari R, Reinikainen K, Kaukoranta E, Hämäläinen M, Ilmoniemi R, Penttinen A, Salminen J, Teszner D (1984): Somatosensory evoked cerebral magnetic fields from SI and SII in man. Electroencephalogr Clin Neurophysiol 57:254–263.

Hari R, Forss N (1999): Magnetoencephalography in the study of human somatosensory cortical processing. Philos Trans R Soc Lond B Biol Sci 354:1145–1154.

Hendry SH, Hsiao SS, Brown MC (1999): Fundamentals of sensory systems. In: Zigmond MJ, Bloom FE, Landis SC, Roberts JL, Squire LR, editor. Fundamental neuroscience. New York: Academic Press. p 657–670.

Hoechstetter K, Rupp A, Meinck HM, Weckesser D, Bornfleth H, Stippich C, Berg P, Scherg M (2000): Magnetic source imaging of tactile input shows task-independent attention effects in SII. Neuroreport 11:2461–2465.

Hubert L, Schultz J (1976): Quadratic assignment as a general data analysis strategy. Br J Math Stat Psychol 29:190–241.

Huttunen J, Ahlfors S, Hari R (1992): Interaction of afferent impulses in the human primary sensorimotor cortex. Electroencephalogr Clin Neurophysiol 82:176–181.

Ioannides AA, Bolton JPR, Clarke CJS (1990): Continuous probabilistic solutions to the biomagnetic inverse problem. Inverse Problem 6:523–542.

Ioannides AA, Liu LC, Kwapien J, Drozdz S, Streit M (2000): Coupling of regional activations in a human brain during an object and face affect recognition task. Hum Brain Mapp 11:77–92.

Iwamura Y, Iriki A, Tanaka M (1994): Bilateral hand representation in the postcentral somatosensory cortex. Nature 369:554–556.

Iwamura Y (1998): Hierarchical somatosensory processing. Curr Opin Neurobiol 8: 522-528.

Jackson ME, Cauller LJ (1998): Neural activity in SII modifies sensory evoked potentials in SI in awake rats. Neuroreport 9:3379–3382.

Jones EG (1985): The thalamus. New York: Plenum Press.

Kaas JH (1990): Somatosensory system. In: Paxinos G, editor. The human nervous system. New York: Academic Press. p 813–844.

Kakigi R, Hoshiyama M, Shimojo M, Naka D, Yamasaki H, Watanabe S, Xiang J, Maeda K, Lam K, Itomi K, Nakamura A (2000): The somatosensory evoked magnetic fields. Prog Neurobiol 61: 495–523.

Kawakami Y, Miyata M, Oshima T (2001): Mechanical vibratory stimulation of feline forepaw skin induces long-lasting potentiation in the secondary somatosensory cortex. Eur J Neurosci 13:171–178.

Karhu J, Tesche CD (1999): Simultaneous early processing of sensory input in human primary (SI) and secondary (SII) somatosensory cortices. J Neurophysiol 81:2017–2025.

Korvenoja A, Huttunen J, Salli E, Pohjonen H, Martinkauppi S, Palva JM, Lauronen L, Virtanen J, Ilmoniemi RJ, Aronen HJ (1999): Activation of multiple cortical areas in response to somatosensory stimulation: combined magnetoencephalographic

and functional magnetic resonance imaging. Hum Brain Mapp 8:13–27.
Krubitzer L, Clarey J, Tweedale R, Elston G, Calford M (1995): A redefinition of somatosensory areas in the lateral sulcus of macaque monkeys. J Neurosci 15:3821–3839.
Laskaris N, Fotopoulos S, Papathanasopoulos P, Bezerianos A (1997): Robust moving averages, with Hopfield neural network implementation, for the monitoring of evoked potential signals. Electroencephalogr Clin Neurophysiol 104:151–156.
Laskaris N, Ioannides AA (2001): Exploratory data analysis of evoked response single trials based on minimal spanning tree. Clin Neurophysiol 112:698–712.
Liu LC, Ioannides AA (1996): A correlation study of averaged and single trial MEG signals: the average describes multiple histories each in a different set of single trials. Brain Topography 8:385–396.
Liu LC, Ioannides AA, Müller-Gärtner HW (1998): Bi-hemispheric study of single trial MEG signals of the human auditory cortex. Electroencephalogr Clin Neurophysiol 106:64–78.
Lopes da Silva F, Van Rotterdam A (1999): Biophysical aspects of EEG and magnetoencephalogram generation. In: Niedermeyer E, Lopes Da Silva F, editors. Electroencephalography: basic principles, clinical applications, and related fields (4th ed). Lippincott: Williams & Wilkins. p 93–109.
Manzoni T, Barbaresi P, Conti F (1984): Callosal mechanism for the interhemispheric transfer of hand somatosensory information in the monkey. Behav Brain Res 11:155–170.
Mauguiere F, Merlet I, Forss N, Vanni S, Jousmaki V, Adeleine P, Hari R (1997): Activation of a distributed somatosensory cortical network in the human brain. A dipole modelling study of magnetic fields evoked by median nerve stimulation. Part I: Location and activation timing of SEF sources. Electroencephalogr Clin Neurophysiol 104:281–289.
Mima T, Nagamine T, Nakamura K, Shibasaki H (1998): Attention modulates both primary and second somatosensory cortical activities in humans: a magnetoencephalographic study. J Neurophysiol 80:2215–2221.
Mountcastle VB (1998): Perceptual neuroscience: the cerebral cortex. Cambridge, MA: Harvard University Press.
Nicolelis MA, Ghazanfar AA, Stambaugh CR, Oliveira LM, Laubach M, Chapin JK, Nelson RJ, Kaas JH (1998): Simultaneous encoding of tactile information by three primate cortical areas. Nat Neurosci 1:621–630.
Ohl FW, Scheich H, Freeman WJ (2001): Change in pattern of ongoing cortical activity with auditory category learning. Nature 412:733–736.
Panzeri S, Petersen RS, Schultz SR, Lebedev M, Diamond ME (2001): The role of spike timing in the coding of stimulus location in rat somatosensory cortex. Neuron 29:769–777.
Paulesu E, Frackowiak R, Bottini G (1997): Maps of somatosensory systems. In: Frackowiak RSJ, Friston KJ, Frith CD, Dolan RJ, Mazziotta JC, editors. Human brain function. London: Academic Press. p 183–242.
Pons TP, Garraghty PE, Mishkin M (1992): Serial and parallel processing of tactual information in somatosensory cortex of rhesus monkeys. J Neurophysiol 68:518–527.
Renyi A (1970): Probability theory. Amsterdam: North Holland.
Recanzone GH (2000): Spatial processing in the auditory cortex of the macaque monkey. Proc Natl Acad Sci USA 97:11829–11835.
Ribary U, Cappell J, Mogilner A, Hund-Georgiadis M, Kronberg E, Llinas R (1999): Functional imaging of plastic changes in the human brain. Adv Neurol 81:49–56.
Riehle A, Grun S, Diesmann M, Aertsen A (1997): Spike synchronization and rate modulation differentially involved in motor cortical function. Science 278:1950–1953.
Romo R, Salinas E (2001): Touch and go: decision-making mechanisms in somatosensation. Annu Rev Neurosci 24:107–137.
Roy SA, Dear SP, Alloway KD (2001): Long-range cortical synchronization without concomitant oscillations in the somatosensory system of anesthetized cats. J Neurosci 21:1795–1808.
Ruben J, Schwiemann J, Deuchert M, Meyer R, Krause T, Curio G, Villringer K, Kurth R, Villringer A (2001): Somatotopic organization of human secondary somatosensory cortex. Cereb Cortex 11:463–473.
Shimojo M, Kakigi R, Hoshiyama M, Koyama S, Kitamura Y, Watanabe S (1996): Intracerebral interactions caused by bilateral median nerve stimulation in man: a magnetoencephalographic study. Neurosci Res 24:175–181.
Simoes C, Hari R (1999): Relationship between responses to contra- and ipsilateral stimuli in the human second somatosensory cortex SII. Neuroimage 10:408–416.
Smith GK, Smith DR (1964): Spike activity in the cerebral cortex. Nature 202:253–255.
Steinmetz PN, Roy A, Fitzgerald PJ, Hsiao SS, Johnson KO, Niebur E (2000): Attention modulates synchronized neuronal firing in primate somatosensory cortex. Nature 404:187–190.
Talairach J, Tournoux P (1988): Co-planar stereotaxic atlas of the human brain. New York: Thieme.
Thompson RF, Spencer WA (1966): Habituation: a model phenomenon for the study of neuronal substrates of behavior. Psychol Rev 73:16–43.
Tsodyks M, Kenet T, Grinvald A, Arieli A (1999): Linking spontaneous activity of single cortical neurons and the underlying functional architecture. Science 286:1943–1946.
Wegner K, Forss N, Salenius S (2000): Characteristics of the human contra- versus ipsilateral SII cortex. Clin Neurophysiol 111:894–900.
Whitsel BL, Petrucelli LM, Werner G (1969): Symmetry and connectivity in the map of the body surface in somatosensory area II of primates. J Neurophysiol 32:170–183.
Yousry TA, Schmid UD, Alkadhi H, Schmidt D, Peraud A, Buettner A, Winkler P (1997): Localization of the motor hand area to a knob on the precentral gyrus. A new landmark. Brain 120:141–157.
Zainos A, Merchant H, Hernandez A, Salinas E, Romo R (1997): Role of primary somatic sensory cortex in the categorization of tactile stimuli: effects of lesions. Exp Brain Res 115:357–360.
Zhang HQ, Zachariah MK, Coleman GT, Rowe MJ (2001): Hierarchical equivalence of somatosensory areas I and II for tactile processing in the cerebral cortex of the marmoset monkey. J Neurophysiol 85:1823–1835.
Zouridakis G, Jansen BH, Boutros NN (1997): A fuzzy clustering approach to EP estimation. IEEE Trans Biomed Eng 44:673–680.